DOI: http://doi.org/10.15446/ing.investig.121139

Research article/Electrical, Electronics, and Telecommunications Engineering

Evaluation of the Accuracy of a Component-Based Aggregated Residential Load Model

Evaluación de la precisión de un modelo agregado de carga residencial basado en componentes

Fabian Rios Gutiérrez[1], Ana Blanco Castañeda[2], Joaquín Caicedo[3], Jan Meyer[4], Andrés Romero Quete[5]

ABSTRACT

Harmonic distortion is one of the most significant electromagnetic disturbances in power systems due to its widespread propagation and well-known adverse effects, including increased energy losses, accelerated equipment aging, and operational failures. In recent years, this disturbance has intensified due to the increasing penetration of power electronic devices (PEDs) in electrical networks, particularly in the residential sector. Although different models have been developed to analyze the individual harmonic behavior of these devices, the models commonly used to represent aggregated residential loads are often simplified and fail to accurately capture their aggregate harmonic behavior. In this paper, based on experimental measurements, Least Squares Estimation (LSE) is used to develop an individual Coupled Norton (CN) model for a typical set of residential loads, which is then used to construct a component-based aggregated model. The accuracy of this aggregated model is evaluated against a measurement-based aggregated model for the same set of PEDs, showing good performance with errors below 10% in the elements of the Frequency Coupling Matrix (FCM). These results indicate that the proposed model is a viable and accurate alternative for representing aggregated residential loads and constitutes a valuable tool for harmonic analysis studies.

Keywords: aggregation methodology, coupled Norton model, harmonics, power quality

RESUMEN

La distorsión armónica es una de las perturbaciones electromagnéticas más relevantes en los sistemas eléctricos, tanto por amplia propagación como por los diversos efectos adversos que puede generar, tales como el aumento de las pérdidas de energía, la aceleración del envejecimiento de los equipos y fallas operativas, entre otros. En los últimos años, esta perturbación se ha intensificado debido al aumento de dispositivos basados en electrónica de potencia (DEPs) en las redes eléctricas, especialmente en el sector residencial. Aunque se han propuesto diferentes enfoques de modelamiento para analizar el comportamiento armónico individual de estos dispositivos, los modelos utilizados para representar cargas residenciales agregadas suelen simplificarse y no logran captar con precisión el comportamiento armónico agregado. En este artículo, a partir de mediciones experimentales y estimación de mínimos cuadrados (MCO), se desarrolla el modelo Norton acoplado individual para un conjunto típico de cargas residenciales, con el cual se construye un modelo agregado basado en componentes. La precisión de este modelo agregado se evalúa frente a un modelo agregado basado en mediciones del mismo conjunto de DEPs, mostrando un buen desempeño con errores inferiores al 10% en los elementos de la matriz acoplada en frecuencia (MAF). Estos resultados indican que el modelo propuesto es una alternativa viable y precisa para la representación de cargas residenciales agregadas, y constituye una herramienta de gran valor para estudios de análisis armónico.

Palabras clave: armónicos, calidad de energía], metodología de agregación, modelo Norton acoplado

Received: November 25th, 2025
Accepted: January 15th, 2026

[1] B.Sc. in Electrical Engineering, Universidad Nacional de Colombia, Colombia. MSc in Electrical Engineering, Universidad Nacional de Colombia, Colombia. Affiliation: PhD student, Instituto de Energía Eléctrica, Universidad Nacional de San Juan, Argentina. Email: fhriosg@unal.edu.co

2 B.Sc. in Electrical Engineering, Universidad Nacional de Colombia, Colombia. MSc in Electrical Engineering, Universidad Nacional de Colombia, Colombia. Ph.D. in Electrical Power Systems, Technische Universität Dresden, Germany. Affiliation: Professor, Institute of Electrical Power Systems and High Voltage Engineering, Technische Universitat Dresden, Germany. Email: ana.blanco@tu-dresden.de

3 B.Sc. in Electrical Engineering, Universidad Distrital Francisco José de Caldas, Colombia. Ph.D. in Electrical Engineering, Universidad Nacional de San Juan, Argentina. Affiliation: MSc student, Universidad Distrital Francisco José de Caldas, Colombia. Email: jecaicedon@udistrital.edu.co

4 B.Sc. in Electrical Engineering, Technische Universität Dresden, Germany. Dipl. in Electrical Power Systems and Ph.D., Technische Universität Dresden, Germany. Affiliation: Professor, Institute of Electrical Power Systems and High Voltage Engineering, Technische Universitat Dresden, Germany. ORCID: https://orcid.org/0000-0002-6884-5101 Email: jan.meyer@tu-dresden.de

5 B.Sc. in Electrical Engineering, Universidad Nacional de Colombia, Colombia. Ph.D in Electrical Engineering, Universidad Nacional de San Juan, Argentina. Affiliation: Professor, Instituto de Energía Eléctrica, Universidad Nacional de San Juan, Argentina. Email: aromero@iee-unsjconicet.org

Introduction

Driven by the growing demand for energy-efficient electrical appliances, the electrification of the residential sector, and ongoing technological advancements, power electronic devices (PEDs) are becoming increasingly prevalent in households. This trend has reached significant proportions; for instance, in Argentina, as of 2018, over 96% of households had at least one television [1], while in Germany, as of 2022, more than 99% of households owned a refrigerator [2]. In the context of electric mobility, it is estimated that by 2025 electric cars will account for over 25% of global car sales [3], further increasing their relevance within residential electricity consumption. Residential photovoltaic (PV) systems, together with battery energy storage systems, have emerged as key tools for increasing user efficiency and enabling households to achieve net-zero energy goals. The expansion of these systems has led residential installations to represent the largest share of newly installed PV capacity in the European Union in 2023 [4]. In addition, emerging technologies aimed at automating previously manual tasks, such as robotic vacuum cleaners, as well as new entertainment devices like smart speakers are further contributing to the increasing number of PEDs per household. This increasing proliferation of PEDs is projected to be one of the main drivers of the rising global electricity demand, which is expected to grow at an average annual rate of 3.4% until 2026 [5].

PEDs operate via electronic interfaces that typically include switched-mode power supplies (SMPS). These interfaces represent a primary source of electromagnetic disturbances, particularly harmonic distortion, in electric power systems. These disturbances degrade power quality (PQ) by causing deviations in voltage and current waveforms from their ideal sinusoidal references [6], [7]. Harmonics, classified as conducted low-frequency phenomena, are among the most critical waveform distortions. According to IEEE definitions, these phenomena are characterized by attributes such as amplitude and frequency [8].

Due to their nonlinear voltage-current behavior, PEDs require specific modeling methodologies for accurately analyzing their effect in electrical networks. These methodologies are generally classified into three categories: time-domain (TD), frequency-domain (FD), and hybrid methods. TD models offer a high degree of accuracy in capturing the nonlinear behavior of PEDs. However, they generally require detailed knowledge of the device and its internal control systems, information that is often not publicly available. These so-called white-box models can be further divided into detailed and averaged models [7], [9]. On the other hand, FD models, while generally less precise, offer a significant advantage in that they are black-box models, not requiring prior knowledge of the device to operate. This category includes the constant current source (CCS) model, the decoupled Norton (DN) model, the coupled Norton (CN) model, and the full Norton (FN) model, all of which are represented by the frequency coupling admittance matrix (FCM) [6], [7], [10], [11], [12]. Hybrid models aim to combine the strengths of both domains and are commonly referred to as grey-box approaches [13].

Due to these advantages, combined with lower computational requirements relative to TD models, FD models are widely used for modeling PEDs and are well-suited for implementation in simulation software. This facilitates a broad range of harmonic studies, including harmonic power flow analysis, determination of harmonic voltage profiles, and sensitivity analysis, among others. These models are typically derived from well-established experimental procedures [14], [15], in which a reference voltage is applied (e.g., sinusoidal voltage without distortion or flat-top voltage waveform) and various harmonic voltages are superimposed one at a time, varying their order, magnitude, and phase, to assess harmonic interactions and cross-coupling phenomena.

As the proliferation of PEDs continues, there is a growing need for accurate aggregated load models to evaluate harmonic behavior in low and medium-voltage networks, including their potential impacts on electrical devices, equipment, and overall power quality levels. Two main approaches have been developed for this purpose: measurement-based and component-based methods. The measurement-based method relies on extensive measurement campaigns conducted at specific nodes or connection points within a group of loads. Consequently, it does not account for the detailed characteristics of the individual loads involved and is therefore classified as a black-box model. This method offers high accuracy, as it captures various operational phenomena and state variations; however, it demands significant resources, lacks flexibility, and is constrained by the temporal and spatial conditions under which the measurements are conducted [16], [17]. In contrast, the component-based method constructs an aggregated model by combining the individual models of each device, which can be obtained through different techniques, including mathematical modeling and measurement-based modeling, among others. This approach offers high flexibility, enabling the analysis of different load compositions, the assessment of regulatory impacts, and the evaluation of technological updates, among other applications. However, modeling each individual device can become excessively complex in large systems, which constitutes its main drawback [18], [19]. While the measurement-based approach captures the behavior of the measured load group regardless of the downstream composition of the measurement point, the component-based approach relies on aggregating individual load models, which can be obtained using various techniques, such as experimental measurements.

Despite the progress achieved in both individual and aggregated harmonic modeling, key questions remain regarding the capability of component-based methodologies to accurately represent the harmonic behavior of residential load groups. In particular, the widespread adoption of PEDs has intensified the need for aggregated models with improved accuracy. This raises an important research question: whether a model with an enhanced capability to represent harmonic behavior, such as the Norton (CN) model, can effectively characterize the aggregated harmonic response of a set of typical residential PEDs, and what level of accuracy can be achieved.

To address this question, this article presents a component-based aggregated model derived through the coupled CN model for a set of four typical residential PEDs. The accuracy of the proposed model is evaluated under the hypothesis that it can capture cross-coupling effects and achieve accuracy comparable to that of a measurement-based aggregated model.

This article is organized as follows: section *Frequency Domain Models* provide an overview of the coupled Norton model. *Experimental Setup and Tested PEDs* describes the experimental procedure used to obtain individual device models, and *Experimental Results* presents the aggregated CN model derived from the selected group of PEDs. A comparative analysis is conducted against a measurement-based model of the same load set, evaluating the accuracy and viability of the proposed approach.

Frequency domain models

The nonlinear voltage–current behavior of PEDs requires linearization of the complex vector function relating these quantities (i.e., the function that defines the current as a response to the applied voltage) around a given operating reference condition, such as an undistorted sinusoidal voltage.

Within the linearization region, harmonic cross-coupling and phase-angle dependence have been modeled using the positive $\bar{\boldsymbol{Y}}^{+}$ and negative $\bar{\boldsymbol{Y}}^{-}$ matrices, as expressed in the well-known full model [6], [7].

Full Norton model – FN model

The FN model is expressed in (1).

$$\bar{\boldsymbol{I}} = \bar{\boldsymbol{I}}_{\boldsymbol{b}} + \bar{\boldsymbol{Y}}^{+}\Delta\bar{\boldsymbol{V}} + \bar{\boldsymbol{Y}}^{-}\Delta\bar{\boldsymbol{V}}^{*} \quad (1)$$

where $\bar{\boldsymbol{I}}_{\boldsymbol{b}}$ is the harmonic current measured under reference conditions. The $\bar{\boldsymbol{Y}}^{+}$matrix represents both the direct and harmonic cross-coupling among different harmonic orders, while $\bar{\boldsymbol{Y}}^{-}$ matrix models the dependence of harmonic currents on harmonic voltage phase angles. These matrices are obtained using a well-established experimental procedure described in the *Experimental Setup and Tested PEDs* section.

The tensor representation is one of the methodologies used to obtain the FN model, in which the $\bar{Y}^{+}$and $\bar{Y}^{-}$ matrices are expressed as compact real-valued matrices whose elements are rank-2 tensors. This approach allows for addressing potential mathematical challenges in the solution of the model matrices [15].

Constant current source model – CCS model

The CCS model is the simplest and most widely used model for representing both individual devices and aggregated loads [12], [18], [20]. It consists of a vector of constant-current sources assumed to be independent of the voltage. The CCS model corresponds to the first term on the right-hand side of (1) and is expressed in (2)

$$\bar{\boldsymbol{I}} = \bar{\boldsymbol{I}}_{\boldsymbol{b}} \quad (2)$$

Decoupled Norton model – DN model

The DN model captures the interaction between the applied harmonic voltages and the resulting harmonic currents of the same order [12]. Accordingly, the model is composed of the diagonal elements of the $\bar{\boldsymbol{Y}}^{+}$ matrix, with the off-diagonal elements set to zero. The model is composed up of the $\bar{\boldsymbol{I}}_{\boldsymbol{b}}$ term and the diagonal of the $\bar{\boldsymbol{Y}}^{+}$matrix from (1), and is expressed in (3).

$$\bar{\boldsymbol{I}} = \bar{\boldsymbol{I}}_{\boldsymbol{b}} + \boldsymbol{diag}(\bar{\boldsymbol{Y}}^{+})\Delta\bar{\boldsymbol{V}} \quad (3)$$

Coupled Norton model – CN model

The CN model captures not only the interactions between voltages and currents of the same harmonic order, but also the cross-coupling between different harmonic orders. This enables a significantly more accurate representation of the harmonic behavior of PEDs, particularly those that exhibit highly nonlinear behavior. The CN model is made up of the $\bar{\boldsymbol{I}}_{\boldsymbol{b}}$ term and $\bar{\boldsymbol{Y}}^{+}$ matrix from (1), and is expressed in (4).

$$\bar{\boldsymbol{I}} = \bar{\boldsymbol{I}}_{\boldsymbol{b}} + \bar{\boldsymbol{Y}}^{+}\Delta\bar{\boldsymbol{V}} \quad (4)$$

Experimental setup and tested PEDs

The experimental procedure involved analyzing the current response of the device under test (DUT) when various harmonic voltages were superimposed on a reference voltage. In this study, the reference voltage corresponded to the undistorted fundamental voltage ($\boldsymbol{V_1 = 230\,V}$). The applied disturbances did not exceed 6% of the fundamental voltage, in accordance with the maximum harmonic voltage limits established by the EN 50160 standard, which specifies a 6% limit for the 5th harmonic order. The phase angle was systematically varied across the complex plane in 30° increments. Harmonic voltages were applied up to the 21st order, considering only odd harmonics. Fig. 1 presents a flowchart summarizing the experimental procedure.

Table 1. PEDs selected for testing

Device	Power	PFC	PF	$\boldsymbol{THD_i}$ (%)
TV LED 50"	77 W	Active	0.87	37.88
Desktop Source	130 W	Active	0.89	25.08
Laptop Charger	65 W	NO	0.41	212.01
CFL	30 W	Active	0.97	17.78

Source: Authors

The experimental procedure described above and illustrated in Fig. 1 was applied to four typical residential loads from key household consumption categories, including lighting, entertainment appliances, and IT equipment. These devices were randomly selected from the laboratory's available resources. In addition, a linear load with a rated power of 120 W was included to account for linear behavior during model development and validation. Further information about these PEDs is provided in Table 1.

Upon completion of the experimental procedure for each individual PED, the same procedure was applied to the entire set of parallel-connected loads. Fig. 2 illustrates the configuration of the experimental setup, which comprised a 15 kVA programmable voltage source, a data acquisition system (DAQ), and a computer used to control the voltage source and measurement devices.

It is worth noting that, within the frequency range considered for the measurements (up to the 21st harmonic order), only voltage values exceeding a threshold of 80 mV were included in the analysis, ensuring measurement uncertainty below 10%, as defined by the measurement system.

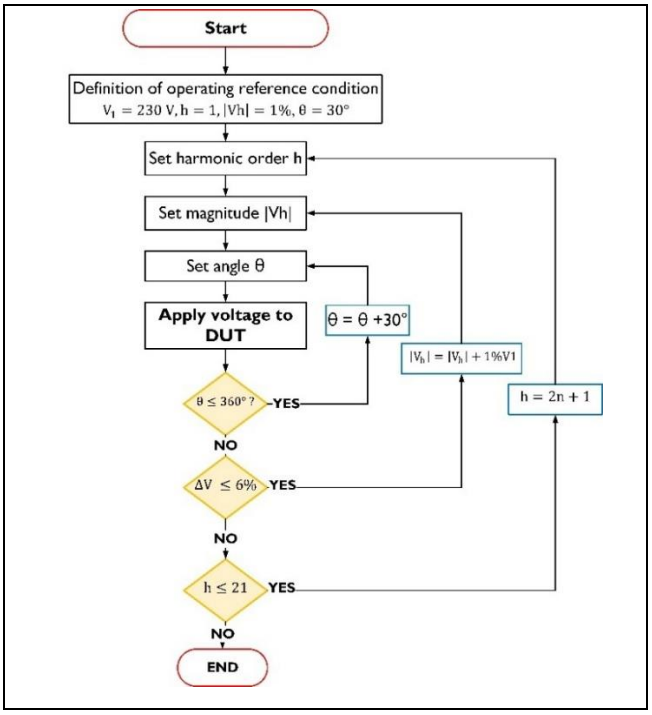

Fig. 1. Flowchart of the experimental procedure
Source: Authors

Model development

Following the experimental procedure described above, a total of 720 measurements were obtained for each individual PED as well as for all loads connected in parallel. Based on these data, the CN model defined in (**4**) was developed.

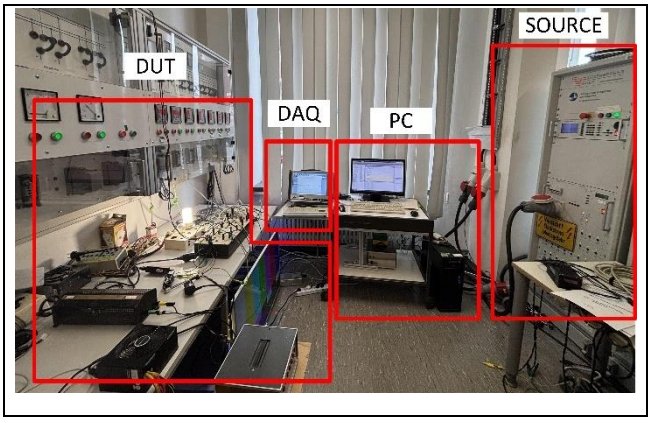

Fig. 2. Test set up
Source: Authors

By expressing (**4**) in the standard linear form given in (**5**), a least squares estimation (LSE) framework was established in which the model minimizes the quadratic error between the measured and predicted current values, as shown in (6). In this formulation, the Frobenius norm extends the LSE method to the matrix case under study:

$$[\bar{I}] = \left[\bar{I}_b \quad \bar{Y}^+\right]\begin{bmatrix}\mathbf{1}\\ \bar{V}\end{bmatrix} \rightarrow \boldsymbol{A} = \boldsymbol{\Theta X} \tag{5}$$

where $A \in \mathbb{C}^{h\times m}$, $\Theta \in \mathbb{C}^{h\times(h+1)}$, $X \in \mathbb{C}^{(h+1)\times m}$, h denotes the harmonic order, and m denotes the number of measurements:

$$\min_{\boldsymbol{\Theta}} \boldsymbol{J}(\boldsymbol{\Theta}) = \|\boldsymbol{I} - \boldsymbol{\Theta X}\|_F^2 \tag{6}$$

Considering the complex matrices involved in the optimization problem, differentiation with respect to $\boldsymbol{\Theta}^*$ yields the general solution expressed in (7):

$$\frac{\partial \boldsymbol{J}}{\partial \boldsymbol{\Theta}^*} = (\boldsymbol{\Theta X} - \boldsymbol{I})\boldsymbol{X}^{\boldsymbol{H}} = \boldsymbol{0} \rightarrow \boldsymbol{\Theta}(\boldsymbol{X}\boldsymbol{X}^{\boldsymbol{H}}) = \boldsymbol{I}\boldsymbol{X}^{\boldsymbol{H}} \tag{7}$$

where $(\cdot)^{\mathbf{H}}$ denotes the conjugate transpose (Hermitian transpose)

Since the number of measurements $\boldsymbol{m}$ is greater than $(\boldsymbol{h}+\mathbf{1})$, the optimal least squares estimator $\widehat{\boldsymbol{\Theta}}$ is defined as expressed in (8):

$$\widehat{\boldsymbol{\Theta}} = \boldsymbol{I}\boldsymbol{X}^{\boldsymbol{H}}(\boldsymbol{X}\boldsymbol{X}^{\boldsymbol{H}})^{-\mathbf{1}} \tag{8}$$

Consequently, the optimal estimator for the CN model is given by (9):

$$[\bar{I}_b \quad \boldsymbol{Y}] = \bar{\boldsymbol{I}}\left(\begin{bmatrix}\mathbf{1}\\ \bar{V}\end{bmatrix}[\mathbf{1} \quad \bar{V}]\right)^{-\mathbf{1}} \tag{9}$$

The first column of the resulting extended matrix represents the current source vector of the CCS model, whereas the remaining columns correspond to the $\bar{Y}^+$ matrix.

The LSE applied in this study allowed for the identification of the parameter values that best represent the voltage-current behavior of the DUT across the measured voltage and frequency ranges.

The proposed modeling methodology enabled the derivation of a CN model for each PED listed in Table 1. The corresponding $\bar{Y}^+$ matrices are presented in Fig. 3. Based on the individual PED models, the aggregated model $\bar{Y}_{AG}^+$ was obtained by the complex phasor summation of the individual $\bar{Y}^+$ matrices from each device up to $\bar{Y}_n^+$, as expressed in (10) and illustrated in Fig. 4.

$$\bar{\boldsymbol{Y}}_{\boldsymbol{AG}}^{+} = \bar{\boldsymbol{Y}}_{\boldsymbol{A}}^{+} + \bar{\boldsymbol{Y}}_{\boldsymbol{B}}^{+} + \cdots + \bar{\boldsymbol{Y}}_{\boldsymbol{n}}^{+} \tag{10}$$

It should also be noted that the same experimental procedure used to obtain the CN models was applied to a linear load to establish an uncertainty threshold. This threshold defines the limit below which the obtained values are considered unreliable and should be disregarded. Based on this analysis, values below 1 μS are considered negligible, as they cannot be reliably associated with the harmonic behavior of the device under test.

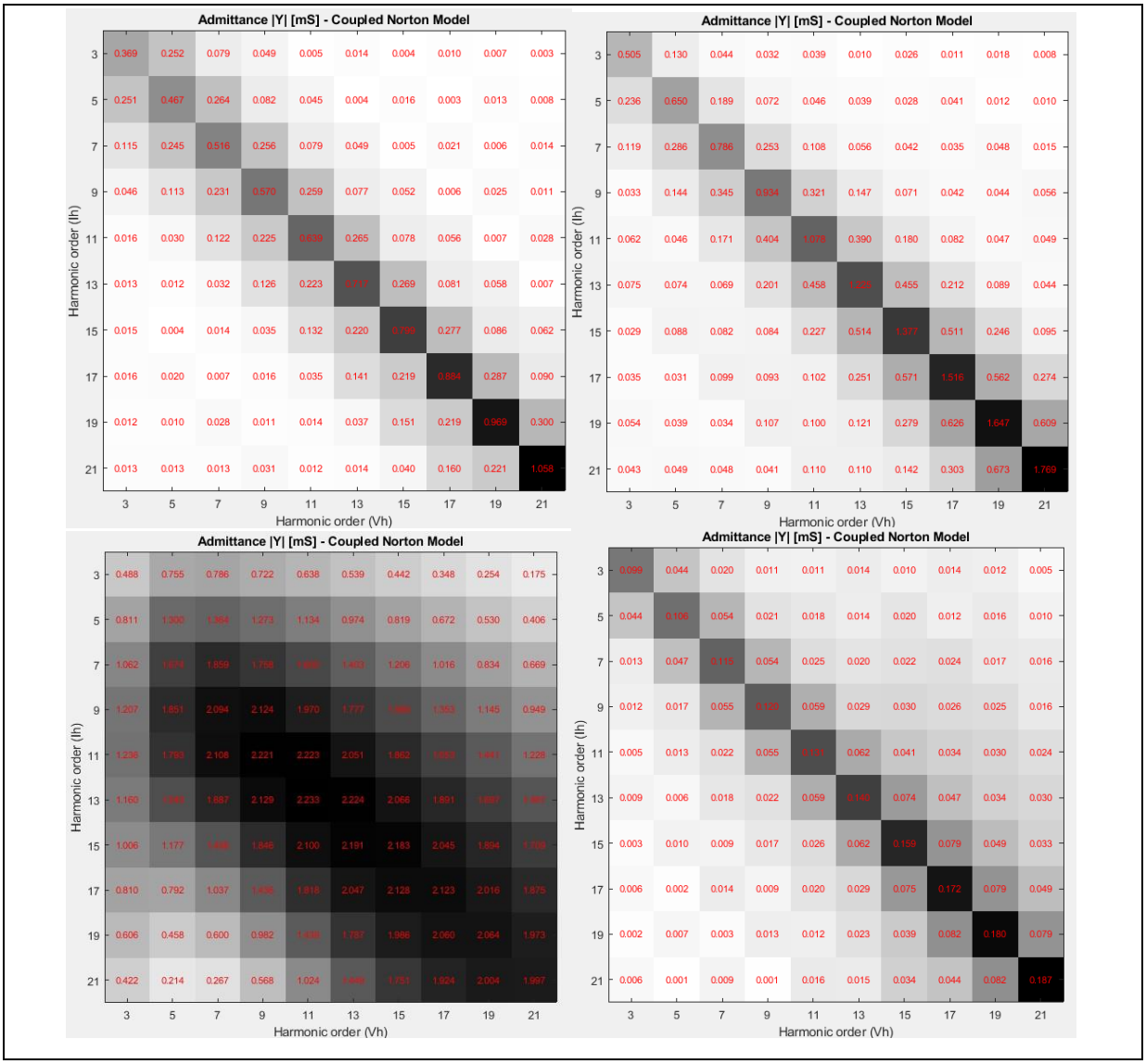

Fig. 3. CN models of PEDs.TV (top left), Desktop (top right), Laptop charger (bottom left), and CFL (bottom right)
Source: Authors

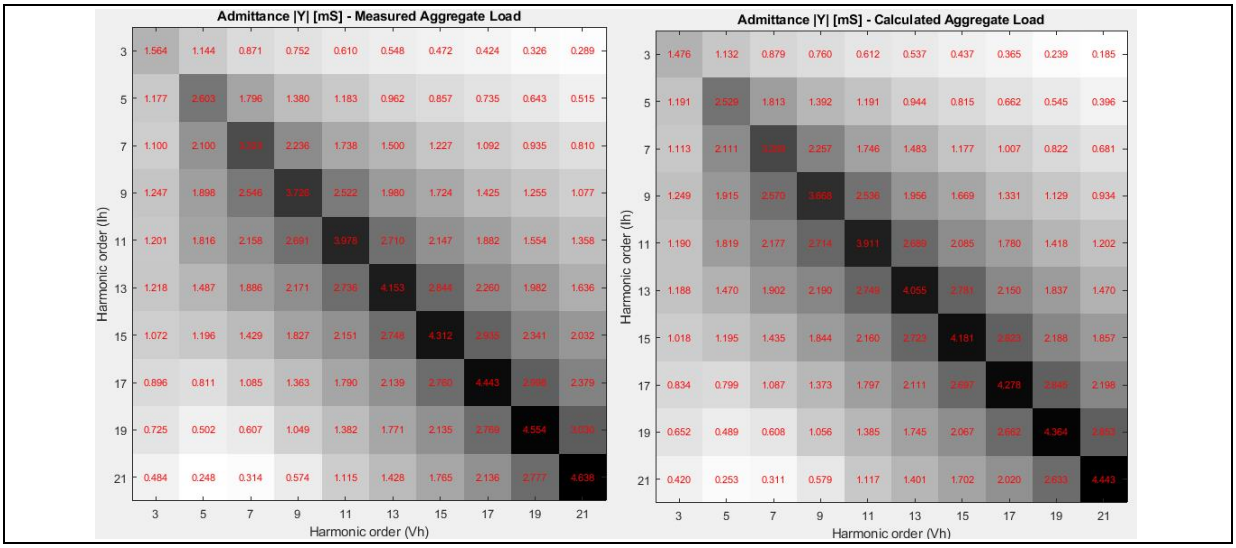

Fig. 4. Measurement-based Aggregated CN model (left) and Component-based Aggregated CN model (right)
Source: Authors

Comparison of the models

The individual models obtained for each device allow for validating the behavior and characteristics described in Table 1. It is evident that for all PEDs, the diagonal elements of the $\overline{Y}^{+}$matrix dominate. This indicates strong coupling between voltage and current harmonic components of the same order. This observation has led some researchers to consider only these diagonal elements when representing the harmonic behavior of PEDs. However, for some PEDs, the off-diagonal elements are comparable in magnitude to the diagonal elements (e.g. PEDs without PFC circuits, such as the laptop charger). Therefore, when modeling aggregate residential loads, which inherently exhibit load variability, it becomes evident that more detailed models than the traditionally used CCS and DN models are required. At the same time, it is essential to maintain the highest possible level of simplicity. For this reason, the CN model was selected for this study.

The individual models also reveal whether a device includes a PFC circuit. For instance, the laptop charger lacks PFC, which account for its high harmonic content, as evidenced by the pronounced off-diagonal components in the model. In contrast, the remaining devices, which are equipped with active PFC, exhibit significantly lower, though not negligible, off-diagonal elements, with magnitudes up to 30% of the maximum diagonal value.

To evaluate the accuracy of the component-based model developed in this study, a comparison was carried out between the magnitude of each element of the admittance matrix obtained from the proposed model (right matrix in Fig. 4) and that obtained from the measurement-based model (left matrix in Fig. 4), using the relative error calculated for each element $\overline{y}_{ij}^{+}$ as expressed in (11). Fig. 5 presents the relative error for each $\overline{y}_{ij}^{+}$ component in matrix form.

The results show that the most significant errors are located on the diagonal, with a maximum of 9.7% for the 3rd and 5th harmonics, and decrease as the harmonic order increases. Off-diagonal component errors are significantly smaller, remaining below 4.5%.

$$e_{ij} = \left| \frac{\overline{y}_{ij-cal}^{+} - \overline{y}_{ij-msr}^{+}}{\overline{y}_{ij-msr}^{+}} \right| \tag{11}$$

The relative error magnitudes are summarized in Fig. 5. To further assess their distribution by harmonic order, Fig. 6 presents the corresponding box plots. That is, it illustrates the error distribution for each harmonic order resulting from the comparison between the component-based model and the measurement-based model. Each box plot shows the distribution of current harmonic order errors for the corresponding voltage harmonic order.

Overall, the range of relative errors decreases as the harmonic order increases. This indicates that lower-order harmonics exhibit higher relative errors, likely due to their greater energy content and consequently higher sensitivity to modeling inaccuracies. It is therefore essential to establish a threshold for when the relative error becomes relevant, based on the study's specific objectives and the required level of model accuracy. Outliers are observed across several harmonic orders, primarily in the diagonal elements and those with the highest magnitudes. For higher-order harmonics, the relative errors tend to be more compact and symmetric, suggesting improved model predictability and stability in that region of the spectrum. Lastly, the median relative error remains within a moderate range across all harmonic orders, with the highest value observed at the third harmonic, approximately 3.5%.

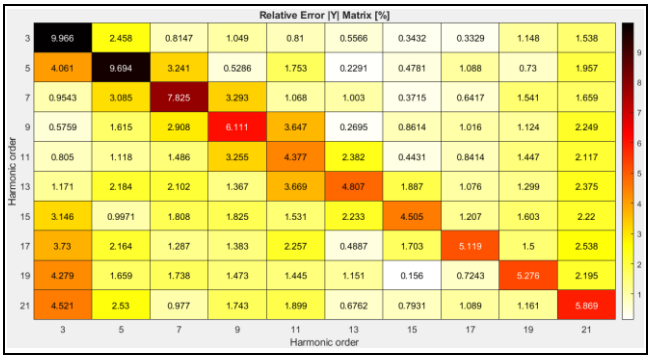

Fig. 5. Relative error of |Y| matrix
Source: Authors

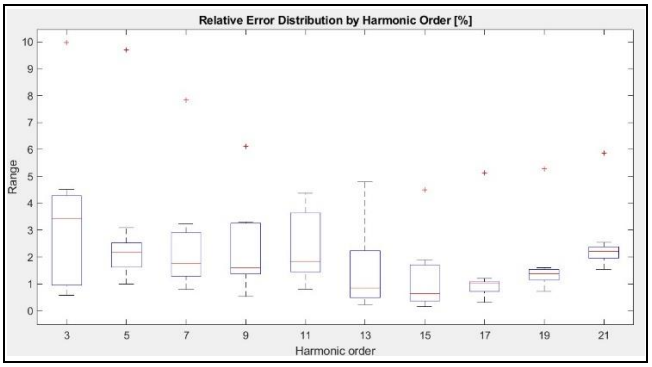

Fig. 6. Relative error by harmonic order
Source: Authors

Discussion

The results obtained in this study were evaluated from two main perspectives: applicability to aggregated modeling and model accuracy. From an applicability standpoint, the proposed approach presents a significant advancement by enabling the aggregation of PEDs with different PFC topologies, overcoming the limitations of reported in previous studies. These include [21], where aggregation was restricted to a single load type (CFLs, PCs, or LCD monitors); [22] and [23], which focused exclusively on the aggregation of PV systems; and [24], in which aggregation was limited to PEDs sharing identical circuit topologies and harmonic behaviors.

In terms of accuracy, the proposed approach exhibits superior performance by incorporating a more comprehensive harmonic representation than those reported in prior studies. In [21], for instance, it was concluded that the DN model was the most accurate formulation, due to the mathematical difficulties associated with other approaches (e.g., the CN and FN models); however, the present study shows that a more detailed formulation can substantially improve the accuracy of the aggregated model. In [22], the CN model was confirmed to provide higher accuracy than simpler alternatives; nevertheless, the methodology reported in that study yields errors approaching 40%, whereas the maximum error in the present study remains below 10%. A further relevant study is presented in [25], which, despite considering the fundamental aspects of aggregated harmonic modeling (both electrical and behavioral), still reproduced approximately 60% of the original data, with performance considerably reduced at higher harmonic orders. This behavior can be attributed, among other factors, to the use of a CCS model, which exhibits inferior accuracy relative to the CN model employed in the present study.

From both computational and experimental perspectives, the proposed approach offers significant advantages. It is shown in [24] that under nominal voltage variations, the maximum error exceeds 10% for large-capacitance rectifier topologies under 20% voltage deviations and for small-capacitance topologies under 40% deviations. Furthermore, [17] highlights the high complexity of fully stochastic measurement-based models, requiring large datasets, the definition of 24-hourly profiles, and the fitting of probability distribution functions for magnitude and phase angle across three user categories (low, medium, and high emission). Although these approaches achieve error rates below 10%, comparable to those obtained in this work, they exhibit lower flexibility and generalization than the proposed model.

Conclusions

Modern residential households increasingly incorporate a growing number of power electronic-based loads, in addition to those acquired in previous years. As a result, the electrical load composition of residential households is characterized by a wide variety of devices with differing topologies, electrical characteristics, applications, manufacturers, and even years of production. This diversity underscores the need for aggregated models that accurately represent the harmonic emissions of these varied loads, both with and without PFC.

Accordingly, this study considered the aggregation of four typical residential loads with distinct harmonic current emission characteristics: three devices equipped with active PFC and one device without PFC. This selection was made to capture both ends of the spectrum: PEDs with optimal harmonic performance (those with active PFC) and those representing worst-case scenarios (devices without PFC).

Under these conditions, a modeling approach is required that goes beyond conventional models such as the widely used DN model, which considers only the direct coupling between voltage and current harmonics of the same order, or the CCS model, which treats each harmonic order independently. For accurate and efficient harmonic representation, it is essential to adopt a model that captures harmonic cross-coupling.

In this regard, the CN model is demonstrated to be an appropriate alternative for both individual and aggregated load modeling, offering a favorable trade-off between computational effort and accuracy. The proposed procedure validated the superior performance of this model not only at the individual device level but also at the aggregated level, addressing the research questions that motivated this study. In addition, the component-based approach provides a high degree of flexibility, allowing the aggregated model to be constructed according to specific configuration requirements, for example, those determined by the time and duration of operation of PEDs within the household, enabling its adaptation to a wide range of residential scenarios.

Consequently, the methodology proposed in this work stands out as a viable and accurate alternative for aggregated harmonic modeling, achieving a maximum element-wise error of 10% or less compared with the measurement-based aggregated model.

This study establishes a foundation for the aggregated modeling of a broader set of residential devices, enabling flexible representation of typical households adapted to different user profiles. Moreover, it opens opportunities for future research that not only considers the harmonic behavior of individual devices but also integrates user behavior, moving towards more comprehensive and realistic modeling frameworks.

Acknowledgements

The authors acknowledge the support of the German Academic Exchange Service (DAAD) through the Third Country Programme Latin America (Grant No. 57587948) and Short-Term Research Scholarship (Grant No. 57760550) for funding this research.

CRediT author statement

Fabian Rios and Ana Maria Blanco: conceptualization, background review, measurements, data collection, and formal analysis. Fabian Rios and Joaquin Caicedo: data processing and validation. Ana Maria Blanco, Jan Meyer, and Andres Romero: workflow development, supervision, and critical review. Fabian Rios: writing — original draft preparation. All authors: writing — review and editing.

Conflicts of interest

The authors declare no conflicts of interest.

Data availability

Data will be available upon request.

Statement on artificial intelligence

During the elaboration of this work, the authors used ChatGPT to improve writing. Following use of this tool, the authors reviewed and edited the content as necessary and take full responsibility for the content of the publication.

References

[1] Instituto Nacional de Estadística y Censos (INDEC), "Encuesta Nacional de Gastos de los Hogares 2017-2018. Uso hogareño de la energía," Buenos Aires, Dec. 2022.

[2] Federal Statistical Office, "Equipment of households with electrical household appliances and others (Germany)," Wiesbaden, 2022.

[3] International Energy Agency (IEA), "Global EV Outlook 2024," Paris, Apr. 2024. Accessed: May 23, 2025. [Online]. Available: https://www.iea.org/reports/global-ev-outlook-2024

[4] SolarPower Europe, "EU Market Outlook for Solar Power 2023–2027," Dec. 2023. Accessed: May 23, 2025. [Online]. Available: https://www.solarpowereurope.org/insights/market-outlooks/eu-market-outlook-for-solar-power-2023-2027

[5] International Energy Agency (IEA), "Electricity 2024. Analysis and forecast to 2026," Jan. 2024. Accessed: May 24, 2025. [Online]. Available: https://www.iea.org/reports/electricity-2024

[6] J. Hernandez, A. A. Romero, S. Muller, and J. Meyer, "Harmonic Distortion in Low Voltage Residential Grids Caused by LED Lamps," in *2022 20th International Conference on Harmonics & Quality of Power (ICHQP)*, Naples, Italy, May 2022, pp. 1–6. https://doi.org/10.1109/ICHQP53011.2022.9808589

[7] A. J. Collin *et al.*, "Analysis of Approaches for Modeling the Low Frequency Emission of LED Lamps," *Energies*, vol. 13, no. 7, p. 1571, Mar. 2020. https://doi.org/10.3390/en13071571

[8] IEEE Standards Association, "IEEE Std 1559 - 2019. Recommended Practice for Monitoring Electric Power

Quality," *IEEE*, Jun. 2019, Accessed: May 23, 2025. [Online]. Available: https://www.iea.org/reports/electricity-2024/executive-summary?utm

[9] A. Reis, A. de L. F. Filho, P. H. F. Moraes, J. P. de Lima, M. S. I. Neto, and V. dos Passos, "Time-domain equivalent model for harmonic simulations of wind and photovoltaic plants," *Electr. Power Syst. Res.*, vol. 235, p. 110727, Oct. 2024. https://doi.org/10.1016/j.epsr.2024.110727

[10] S. Müller, J. Meyer, and P. Schegner, "Extended coupled Norton model of modern power-electronic devices for large-scale harmonic studies in distribution networks," *IET Power Electron.*, vol. 13, no. 13, pp. 2706–2714, Oct. 2020. https://doi.org/10.1049/iet-pel.2019.1444

[11] M. Ramzan, A. Othman, and N. R. Watson, "Comparison of assessment methods for tensors of nonlinear devices," *Electr. Power Syst. Res.*, vol. 219, p. 109237, Jun. 2023. https://doi.org/10.1016/j.epsr.2023.109237

[12] X. Xie, J. Zhang, Y. Sun, and J. Fan, "A Measurement-Based Dynamic Harmonic Model for Single-Phase Diode Bridge Rectifier-Type Devices," *IEEE Trans. Instrum. Meas.*, vol. 73, art. 9001313, 2024. https://doi.org/10.1109/TIM.2024.3370782

[13] X. Xu *et al.*, "Evaluation of hybrid harmonic modelling techniques: Case study of harmonic interactions of EVs and CFLs," in *2016 IEEE PES Innovative Smart Grid Technologies Conference Europe (ISGT-Europe)*, IEEE, Oct. 2016, pp. 1–6. https://doi.org/10.1109/ISGTEurope.2016.7856296

[14] J. Yadav, K. Vasudevan, J. Meyer, and D. Kumar, "Frequency Coupling Matrix Model of a Three-Phase Variable Frequency Drive," *IEEE Trans. Ind. Appl.*, vol. 58, no. 3, pp. 3652–3663, May 2022. https://doi.org/10.1109/TIA.2022.3156104

[15] J. E. Caicedo, A. A. Romero, H. C. Zini, R. Langella, J. Meyer, and N. R. Watson, "Impact of reference conditions on the frequency coupling matrix of a plug-in electric vehicle charger," in *2018 18th International Conference on Harmonics and Quality of Power (ICHQP)*, IEEE, May 2018, pp. 1–6. https://doi.org/10.1109/ICHQP.2018.8378898

[16] M. T. Au and J. V. Milanović, "Development of stochastic aggregate harmonic load model based on field measurements," *IEEE Trans. Power Del.*, vol. 22, no. 1, pp. 323–330, Jan. 2007. https://doi.org/10.1109/TPWRD.2006.881455

[17] A. M. Blanco, A. Grevener, S. Müller, J. Meyer, and P. Schegner, "Stochastic harmonic load model of residential users based on measurements," in *2015 IEEE Eindhoven PowerTech*, Jun. 2015, pp. 1–6. https://doi.org/10.1109/PTC.2015.7232634

[18] P. Rodríguez-Pajarón, E. Caro, A. Hernández, and M. Izzeddine, "A Bottom-up model for simulating residential harmonic injections," *Energy Build.*, vol. 265, p. 112103, Jun. 2022. https://doi.org/10.1016/j.enbuild.2022.112103

[19] Y. Sun, X. Xie, Q. Wang, L. Zhang, Y. Li, and Z. Jin, "A bottom-up approach to evaluate the harmonics and power of home appliances in residential areas," *Appl. Energy*, vol. 259, p. 114207, Feb. 2020. https://doi.org/10.1016/j.apenergy.2019.114207

[20] M. Ishaq and R. Langella, "Aggregated Load Modelling Approach to Study Impact of Heat Pumps Harmonic Distortion on the Low Voltage Distribution Network," *J. Eur. Syst. Autom.*, vol. 57, no. 5, pp. 1497–1502, Oct. 2024. https://doi.org/10.18280/jesa.570525

[21] A. B. Nassif, J. Yong, and W. Xu, "Measurement-based approach for constructing harmonic models of electronic home appliances," *IET Gener. Transm. Distrib.*, vol. 4, no. 3, pp. 363–375, 2010. https://doi.org/10.1049/iet-gtd.2009.0240

[22] A. Martínez-Peñaloza and G. Osma-Pinto, "Analysis of the Performance of the Norton Equivalent Model of a Photovoltaic System Under Different Operating Scenarios," *Int. Rev. Electr. Eng.*, vol. 16, no. 4, p. 328, Aug. 2021. https://doi.org/10.15866/iree.v16i4.20278

[23] X. Xu *et al.*, "Aggregate harmonic fingerprint models of PV inverters. part 1: Operation at different powers," in *2018 18th International Conference on Harmonics and Quality of Power (ICHQP)*, Ljubljana, Slovenia, May 2018, pp. 1–6. https://doi.org/10.1109/ICHQP.2018.8378824

[24] A. S. Fölting, J. M. A. Myrzik, T. Wiesner, and L. Jendernalik, "Practical implementation of the coupled Norton approach for nonlinear harmonic models," in *Power Systems Computation Conference*, 2014. https://doi.org/10.1109/PSCC.2014.7038372

[25] D. Salles, C. Jiang, W. Xu, W. Freitas, and H. E. Mazin, "Assessing the collective harmonic impact of modern residential loads-part I: Methodology," *IEEE Trans. Power Del.*, vol. 27, no. 4, pp. 1937–1946, 2012. https://doi.org/10.1109/TPWRD.2012.2207132